arXiv:0805.2777v2 [hep-th] 3 Jul 2008

Non-contact gears: II. Casimir torque between concentric corrugated cylinders for the scalar case

Inés Cavero-Peláez*
Laboratoire Kastler Brossel, Université Pierre et Marie Curie, ENS, CNRS,
Campus Jussieu, University Paris 6, Case 74, F-75252 Paris, cedex 05, France.

Kimball A. Milton,† Prachi Parashar,‡ and K. V. Shajesh§
Oklahoma Center for High Energy Physics and Homer L. Dodge Department of Physics and Astronomy,
University of Oklahoma, Norman, OK 73019, USA.

(Dated: July 3, 2008)

The Casimir interaction between two concentric corrugated cylinders provides the mechanism for non-contact gears. To this end, we calculate the Casimir torque between two such cylinders, described by δ-potentials, which interact through a scalar field. We derive analytic expressions for the Casimir torque for the case when the corrugation amplitudes are small in comparison to the corrugation wavelengths. We derive explicit results for the Dirichlet case, and exact results for the weak coupling limit, in the leading order. The results for the corrugated cylinders approach the corresponding expressions for the case of corrugated parallel plates in the limit of large radii of cylinders (relative to the difference in their radii) while keeping the corrugation wavelength fixed.

I. INTRODUCTION

The Casimir torque between two material bodies, which is the rotational analog of the Casimir force [1], was studied for the first time in 1973 [2]. The Casimir torque between two uni-axial birefringent dielectric plates has been studied more recently in [3]. The lateral Casimir force between corrugated parallel plates was calculated perturbatively in [4].

Lately a non-contact rack and pinion arrangement has been proposed in [5] and discussed in the proximity force approximation (PFA) limit. This proposal has been generalized to the design of a non-contact gear consisting of two corrugated concentric cylinders in [6] to discuss possible experimental arrangements. The perturbative calculation for the Casimir torque between two concentric corrugated cylinders, in the spirit of [4], has not yet been carried out. We achieve this task to the leading order for the scalar case here. The next-to-leading-order calculation for the corrugated cylinders, in the spirit of the corresponding case of corrugated plates [7], is in progress.

A. Statement of the problem

We consider two concentric, semi-transparent, corrugated cylinders described by the potentials,

$$V_i(r,\theta) = \lambda_i \, \delta(r - a_i - h_i(\theta)), \tag{1}$$

where $i = 1, 2$ are labels that identify the individual cylinders, and we shall have $a = a_2 - a_1 > 0$. The functions $h_i(\theta)$ describe the corrugations associated with the cylinders. We define the function

$$a(\theta) = a + h_2(\theta) - h_1(\theta), \tag{2}$$

which measures the relative corrugations between the cylinders. We shall define the corrugations $h_i(\theta)$ such that the mean of the relative corrugations evaluates to a,

$$\frac{1}{2\pi} \int_0^{2\pi} d\theta \left[h_2(\theta) - h_1(\theta) \right] = 0. \tag{3}$$

---

*Electronic address: Ines.Cavero-Pelaez@spectro.jussieu.fr
†Electronic address: milton@nhn.ou.edu; URL: `http://www.nhn.ou.edu/%7Emilton`
‡Electronic address: prachi@nhn.ou.edu
§Electronic address: shajesh@nhn.ou.edu; URL: `http://www.nhn.ou.edu/%7Eshajesh`

Let E be the total Casimir energy associated with the two concentric corrugated cylinders, including the divergent contributions associated with the single cylinders. In general this energy changes if we rotate one of the cylinders with respect to the other and thus leads to a torque between the cylinders. This shift can be described by an angular rotation, θ_0, of the corrugations on the inner cylinder as $h_1(\theta+\theta_0)$ and the corresponding torque will be

$$\mathcal{T} = -\frac{\partial E}{\partial \theta_0}. \tag{4}$$

We observe that due to rotational symmetry there will be no torque between two uncorrugated cylinders. Further, using the same argument there will be no torque when only one of the cylinders has corrugations on it. In light of these observations it is helpful to write the total Casimir energy for two corrugated concentric cylinders in the form

$$E = E^{(0)} + E_1 + E_2 + E_{12}(\theta_0), \tag{5}$$

where, $E^{(0)}$ is the energy of the configuration when the corrugations are absent on both the cylinders, E_i is the additional contribution to the Casimir energy when one of the cylinders is uncorrugated, and E_{12} is the contribution to the energy which is present only when both cylinders are corrugated. Thus, E_{12} is the interaction energy due to the presence of corrugation, and only this term in eq. (5) contributes to the torque between the cylinders. The physical quantities associated with the uncorrugated cylinders thus act as a background, and a reference, and we shall find it convenient to denote them by the superscript (0) to mean zeroth order. The potential for the background is

$$V_i^{(0)}(r) = \lambda_i \delta(r-a_i), \tag{6}$$

which has no angular dependence.

Using the multiple scattering formalism, see [8, 9] and references in [9], which has been further discussed for the case of corrugated plates in [7], we can write

$$\Delta E = E_1 + E_2 + E_{12}, \tag{7}$$

where in accordance with the notation given in [7], ΔX represents the deviation of the physical quantity, X, from the background. The term in eq. (7) which contributes to the Casimir torque, to the leading order, is given by [7]

$$E_{12}^{(2)} = \frac{i}{2\mathcal{T}} \,\mathrm{Tr}\Big[G^{(0)}\Delta V_1^{(1)} G^{(0)} \Delta V_2^{(1)}\Big], \tag{8}$$

where the Green's function associated with the background satisfies the differential equation,

$$\Big[-\partial^2 + V_1^{(0)} + V_2^{(0)}\Big] G^{(0)} = 1. \tag{9}$$

In the leading order the corrugations are treated as small perturbations, $|h_i(\theta)| \ll a < a_i$, which lets us approximate the potentials by

$$\Delta V_i(r,\theta) \approx V_i^{(1)}(r,\theta) = h_i(\theta) \frac{\partial}{\partial r} V_i^{(0)}(r), \tag{10}$$

where we have used the superscript (1) to represent the first order perturbation in the quantity.

II. GREEN'S FUNCTION

We observe that the evaluation of the interaction energy, E_{12}, to the leading order, involves solving for the Green's function for the configuration involving the background alone. This amounts to solving the differential equation in eq. (9), whose solution can be written as

$$G^{(0)}(x,x') = \int \frac{d\omega}{2\pi} e^{-i\omega(t-t')} \int \frac{dk}{2\pi} e^{ik(z-z')} \sum_{m=-\infty}^{\infty} \frac{1}{2\pi} e^{im(\theta-\theta')} g_m^{(0)}(r,r';\kappa), \tag{11}$$

where $\kappa^2 = k^2 - \omega^2$. The reduced Green's function, $g_m^{(0)}(r,r';\kappa)$, satisfies the equation

$$-\left[\frac{1}{r}\frac{\partial}{\partial r} r \frac{\partial}{\partial r} - \frac{m^2}{r^2} - \kappa^2 - \lambda_1 \delta(r-a_1) - \lambda_2 \delta(r-a_2)\right] g_m^{(0)}(r,r';\kappa) = \frac{\delta(r-r')}{r}. \tag{12}$$

The solution for $g_m^{(0)}(r,r';\kappa)$ in the above equation is expressed in terms of the modified Bessel functions as

$$g_m^{(0)}(r,r';\kappa) = \begin{cases} I_m(\kappa r_<)K_m(\kappa r_>) - \frac{1}{\Delta}\big[\lambda_1 a_1 \lambda_2 a_2\, K_1 K_2 \left(I_2 K_1 - I_1 K_2\right) \\ \qquad\qquad + \lambda_1 a_1\, K_1^2 + \lambda_2 a_2\, K_2^2\big]\, I_m(\kappa r) I_m(\kappa r'), & \text{if} \quad (r,r') < a_1 < a_2, \\ I_m(\kappa r_<)K_m(\kappa r_>) + \frac{1}{\Delta}\big[-\lambda_2 a_2\, K_2^2 \left(1 + \lambda_1 a_1\, I_1 K_1\right)\big]\, I_m(\kappa r) I_m(\kappa r') \\ \qquad + \frac{1}{\Delta}\big[-\lambda_1 a_1\, I_1^2 \left(1 + \lambda_2 a_2\, I_2 K_2\right)\big]\, K_m(\kappa r) K_m(\kappa r') \\ \qquad + \frac{1}{\Delta}\big[\lambda_1 a_1 \lambda_2 a_2\, I_1^2 K_2^2\big]\, I_m(\kappa r) K_m(\kappa r') \\ \qquad + \frac{1}{\Delta}\big[\lambda_1 a_1 \lambda_2 a_2\, I_1^2 K_2^2\big]\, K_m(\kappa r) I_m(\kappa r'), & \text{if} \quad a_1 < (r,r') < a_2, \\ I_m(\kappa r_<)K_m(\kappa r_>) - \frac{1}{\Delta}\big[\lambda_1 a_1 \lambda_2 a_2\, I_1 I_2 \left(I_2 K_1 - I_1 K_2\right) \\ \qquad\qquad + \lambda_1 a_1\, I_1^2 + \lambda_2 a_2\, I_2^2\big]\, K_m(\kappa r) K_m(\kappa r'), & \text{if} \quad a_1 < a_2 < (r,r'), \\ \frac{1}{\Delta}\big[1 + \lambda_2 a_2\, I_2 K_2\big]\, I_m(\kappa r) K_m(\kappa r') - \frac{1}{\Delta}\big[\lambda_2 a_2\, K_2^2\big]\, I_m(\kappa r) I_m(\kappa r'), & \text{if} \quad r < a_1 < r' < a_2, \\ \frac{1}{\Delta}\, I_m(\kappa r) K_m(\kappa r'), & \text{if} \quad r < a_1 < a_2 < r', \\ \frac{1}{\Delta}\big[1 + \lambda_1 a_1\, I_1 K_1\big]\, I_m(\kappa r) K_m(\kappa r') - \frac{1}{\Delta}\big[\lambda_1 a_1\, I_1^2\big]\, K_m(\kappa r) K_m(\kappa r'), & \text{if} \quad a_1 < r < a_2 < r', \end{cases} \tag{13}$$

where we have used the abbreviation

$$\Delta = 1 + \lambda_1 a_1\, I_1 K_1 + \lambda_2 a_2\, I_2 K_2 + \lambda_1 a_1 \lambda_2 a_2\, I_1 K_2 \left(I_2 K_1 - I_1 K_2\right). \tag{14}$$

We have used the notation $I_{1,2} \equiv I_m(\kappa a_{1,2})$ and $K_{1,2} \equiv K_m(\kappa a_{1,2})$. In the other regions not quoted above the solution is determined by using the reciprocal symmetry, $g_m^{(0)}(r,r';\kappa) = g_m^{(0)}(r',r;\kappa)$, in the Green's function.

Using the above expressions we can evaluate

$$g_m^{(0)}(a_1,a_2;\kappa) = \frac{1}{\Delta}\, I_1 K_2. \tag{15}$$

The relevant first derivatives are evaluated using the averaging prescription described in [7], which is not necessary in either the Dirichlet or weak limit, as

$$\left\{\frac{\partial}{\partial r} g_m^{(0)}(r,r';\kappa)\right\}_{r=a_1,r'=a_2} = \frac{\kappa}{\Delta}\left[I_1' K_2 + \frac{\lambda_1}{2\kappa}\, I_1 K_2\right], \tag{16a}$$

$$\left\{\frac{\partial}{\partial r} g_m^{(0)}(r,r';\kappa)\right\}_{r=a_2,r'=a_1} = \frac{\kappa}{\Delta}\left[I_1 K_2' - \frac{\lambda_2}{2\kappa}\, I_1 K_2\right], \tag{16b}$$

where we have used a prime to denote the derivative of the modified Bessel function with respect to the argument. The derivatives acting on the second variable in the Green's can be deduced using the symmetry of the Green's function. The relevant second derivatives are evaluated to be

$$\left\{\frac{\partial}{\partial r}\frac{\partial}{\partial r'} g_m^{(0)}(r,r';\kappa)\right\}_{r=a_1,r'=a_2} = \frac{\kappa^2}{\Delta}\left[I_1' K_2' + \frac{\lambda_1}{2\kappa}\, I_1 K_2' - \frac{\lambda_2}{2\kappa}\, I_1' K_2 - \frac{\lambda_1}{2\kappa}\frac{\lambda_2}{2\kappa}\, I_1 K_2\right]. \tag{17}$$

The above evaluations used the Wronskian, $[I_m(x)K_m'(x) - I_m'(x)K_m(x)] = -1/x$, satisfied by the modified Bessel functions.

III. INTERACTION ENERGY

In terms of the reduced Green's function defined in eq. (13) we can write the interaction energy, to the leading order, in eq. (8) as

$$\frac{E_{12}^{(2)}}{L_z} = \frac{1}{(2\pi)^2} \sum_{m=-\infty}^{\infty} \sum_{n=-\infty}^{\infty} (\tilde{h}_1)_{m-n} (\tilde{h}_2)_{n-m}\, L_{mn}^{(2)}, \tag{18}$$

where $(\tilde{h}_i)_m$ are the Fourier transforms of the functions $h_i(\theta)$, which describe the corrugations on the cylinders, and are defined as

$$(\tilde{h}_i)_m = \int_0^{2\pi} d\theta \, e^{-im\theta} \, h_i(\theta). \tag{19}$$

The matrix (or the kernel) $L^{(2)}_{mn}$ in eq. (18) is expressed in the form

$$L^{(2)}_{mn} = -\frac{1}{4\pi} \int_0^\infty \kappa \, d\kappa \, I^{(2)}_{mn}(a_1, a_2; \kappa), \tag{20}$$

where $\kappa^2 = k_z^2 - \omega^2 = k_z^2 + \zeta^2$, after switching to imaginary frequencies by a Euclidean rotation, $\omega \to i\zeta$. The related matrix $I^{(2)}_{mn}(a_1, a_2; \kappa)$ is expressed as derivatives of the reduced Green's function in the form

$$I^{(2)}_{mn}(a_1, a_2; \kappa) = \lambda_1 \lambda_2 \frac{\partial}{\partial r} \frac{\partial}{\partial \bar{r}} \Big[r \, \bar{r} \, g^{(0)}_m(r, \bar{r}; \kappa) \, g^{(0)}_n(\bar{r}, r; \kappa) \Big] \bigg|_{\bar{r}=a_1, r=a_2}. \tag{21}$$

The reciprocal symmetry in the Green's function leads to the following symmetry in the above kernel:

$$I^{(2)}_{mn}(a_1, a_2; \kappa) = I^{(2)}_{nm}(a_2, a_1; \kappa). \tag{22}$$

The expression in eq. (21) is evaluated using eqs. (15), (16), and (17):

$$\begin{aligned} I^{(2)}_{mn}(a_1, a_2; \kappa) \;=\; \frac{\lambda_1 \lambda_2}{\Delta \tilde{\Delta}} \bigg[& I_1 K_2 \, \tilde{I}_1 \tilde{K}_2 + \kappa a_1 \, I_1 K_2 \left(\tilde{I}_1' \tilde{K}_2 + \frac{\lambda_1}{2\kappa} \, \tilde{I}_1 \tilde{K}_2 \right) + \kappa a_1 \left(I_1' K_2 + \frac{\lambda_1}{2\kappa} \, I_1 K_2 \right) \tilde{I}_1 \tilde{K}_2 \\ & + \kappa a_2 \, I_1 K_2 \left(\tilde{I}_1 \tilde{K}_2' - \frac{\lambda_2}{2\kappa} \, \tilde{I}_1 \tilde{K}_2 \right) + \kappa a_2 \left(I_1 K_2' - \frac{\lambda_2}{2\kappa} \, I_1 K_2 \right) \tilde{I}_1 \tilde{K}_2 \\ & + \kappa a_1 \kappa a_2 \left(I_1 K_2' - \frac{\lambda_2}{2\kappa} \, I_1 K_2 \right) \left(\tilde{I}_1' \tilde{K}_2 + \frac{\lambda_2}{2\kappa} \, \tilde{I}_1 \tilde{K}_2 \right) \\ & + \kappa a_1 \kappa a_2 \left(I_1' K_2 + \frac{\lambda_1}{2\kappa} \, I_1 K_2 \right) \left(\tilde{I}_1 \tilde{K}_2' - \frac{\lambda_2}{2\kappa} \, \tilde{I}_1 \tilde{K}_2 \right) \\ & + \kappa a_1 \kappa a_2 \left(I_1' K_2' + \frac{\lambda_1}{2\kappa} \, I_1 K_2' - \frac{\lambda_2}{2\kappa} \, I_1' K_2 - \frac{\lambda_1}{2\kappa} \frac{\lambda_2}{2\kappa} \, I_1 K_2 \right) \tilde{I}_1 \tilde{K}_2 \\ & + \kappa a_1 \kappa a_2 \, I_1 K_2 \left(\tilde{I}_1' \tilde{K}_2' + \frac{\lambda_1}{2\kappa} \, \tilde{I}_1 \tilde{K}_2' - \frac{\lambda_2}{2\kappa} \, \tilde{I}_1' \tilde{K}_2 - \frac{\lambda_1}{2\kappa} \frac{\lambda_2}{2\kappa} \, \tilde{I}_1 \tilde{K}_2 \right) \bigg], \end{aligned} \tag{23}$$

where we have used the notation in which the modified Bessel function with a tilde on it is of order n and that without a tilde is of order m. The tilde on Δ means that we use the corresponding modified Bessel functions in eq. (14).

A. Dirichlet Limit

For the case of the Dirichlet limit ($a\lambda_{1,2} \gg 1$) the expression in eq. (23) takes the relatively simple form

$$I^{(2)D}_{mn}(a_1, a_2; \kappa) = -\frac{1}{a_1 a_2} \frac{1}{[I_2 K_1 - I_1 K_2]} \frac{1}{[\tilde{I}_2 \tilde{K}_1 - \tilde{I}_1 \tilde{K}_2]} = -\frac{1}{a_1 a_2} \frac{1}{D_m(\alpha; \kappa R)} \frac{1}{D_n(\alpha; \kappa R)} \tag{24}$$

where the superscript D stands for Dirichlet, and for convenience we have introduced the function

$$D_m(\alpha; x) = I_m\big(x[1+\alpha]\big) K_m\big(x[1-\alpha]\big) - I_m\big(x[1-\alpha]\big) K_m\big(x[1+\alpha]\big), \tag{25}$$

and two related variables: $R = (a_1 + a_2)/2$, which is the mean radius of the two cylinders under consideration, and $\alpha = a/2R$, which by definition is less than unity. We note that

$$\frac{a^2}{a_1 a_2} = \frac{4\,\alpha^2}{(1-\alpha^2)}. \tag{26}$$

Two cylinders with very large radius, such that $a_i \to \infty$ with a kept fixed, will simulate a parallel plate in the region of small variations in the angle ($\theta \to 0$). This corresponds to $m, n \to \infty$, such that m/R is finite and $\alpha \to 0$.

These limits are compatible with the leading uniform asymptotic approximants to the modified Bessel functions for large orders, see for eg. [10],

$$I_m(mz) \sim \sqrt{\frac{t}{2\pi m}}\, e^{m\eta(z)} \qquad \text{and} \qquad K_m(mz) \sim \sqrt{\frac{\pi t}{2m}}\, e^{-m\eta(z)}, \qquad m \to \infty, \tag{27}$$

where

$$t = \frac{1}{\sqrt{1+z^2}} \qquad \text{and} \qquad \eta(z) = \sqrt{1+z^2} + \ln \frac{z}{1+\sqrt{1+z^2}}. \tag{28}$$

Using the above asymptotic behaviors and neglecting terms of order α we can deduce, for large order m,

$$\frac{4\,\alpha^2}{(1-\alpha^2)} \frac{1}{D_m(\alpha;\kappa R)} \frac{1}{D_n(\alpha;\kappa R)} \sim \frac{\kappa_m a}{\sinh \kappa_m a} \frac{\kappa_n a}{\sinh \kappa_n a}, \tag{29}$$

where we have denoted $\kappa_m^2 = \kappa^2 + (m/R)^2$ and $\kappa_n^2 = \kappa^2 + (n/R)^2$. Using the above limiting form in eq. (24), and after interpreting $m/R \to k$ as the Fourier transform of the coordinate containing the corrugations on the plates, we reproduce the expression derived for the corrugated plates in [7].

Using eq. (24) in eq. (20) the L-matrix in the Dirichlet limit takes the form

$$L_{mn}^{(2)D} = \frac{1}{a^2} \frac{1}{4\pi} \int_0^\infty \kappa\, d\kappa \frac{a^2}{a_1 a_2} \frac{1}{D_m(\alpha;\kappa R)} \frac{1}{D_n(\alpha;\kappa R)}, \tag{30}$$

which also leads to the corresponding result for the corrugated plates.

B. Weak coupling Limit

For the case of weak coupling limit ($a\lambda_{1,2} \ll 1$) the expression in eq. (23) takes the form

$$I_{mn}^{(2)W}(a_1, a_2; \kappa) = \lambda_1 \lambda_2 \frac{\partial}{\partial a_1} a_1 \frac{\partial}{\partial a_2} a_2 \Big[I_m(\kappa a_1) K_m(\kappa a_2) I_n(\kappa a_1) K_n(\kappa a_2) \Big], \tag{31}$$

where W stands for weak coupling limit. Using the above expression for I-matrix in eq. (20) we can write the L-matrix in the weak coupling limit as

$$L_{mn}^{(2)W} = -\frac{\lambda_1 \lambda_2}{4\pi} \frac{\partial}{\partial a_1} a_1 \frac{\partial}{\partial a_2} \frac{1}{a_2} F_{mn}\Big(\frac{a_1}{a_2}\Big), \tag{32}$$

where we have introduced the function

$$F_{mn}(\beta) = \int_0^\infty x\, dx\, K_m(x) K_n(x) I_m(\beta x) I_n(\beta x). \tag{33}$$

Taking the uniform asymptotic approximants of the modified Bessel functions, see eq. (27), in the above expression, we can reproduce the corresponding result for the corrugated plates in [7].

It is possible to convert the above integral into a single sum using the technique described in [9]. We replace those modified Bessel functions which are well defined at the origin, I_m, with their power series expansions, then perform the integral using

$$\int_0^\infty x\, dx\, x^{m+n+2k} K_m(x) K_n(x) = \frac{1}{2} \frac{2^{m+n+2k}(m+n+2k+1)!}{k!(k+m)!(k+n)!(k+m+n)!}, \qquad m \geq 0, n \geq 0, k \geq 0, \tag{34}$$

which leaves eq. (33) in terms of two sums. One of the sums can be performed after regrouping the terms, and leads to

$$\begin{aligned} F_{mn}(\beta) &= \frac{1}{2} \beta^{m+n} \sum_{k=0}^\infty \beta^{2k} \frac{1}{(m+n+2k+1)!} \sum_{k'=0}^{k} \frac{k!(k+m)!(k+n)!(k+m+n)!}{k'!(k'+m)!(k-k')!(k-k'+n)!} \\ &= \frac{1}{2} \sum_{k=0}^\infty \frac{\beta^{2k+m+n}}{(2k+m+n+1)}, \qquad m \geq 0, n \geq 0. \end{aligned} \tag{35}$$

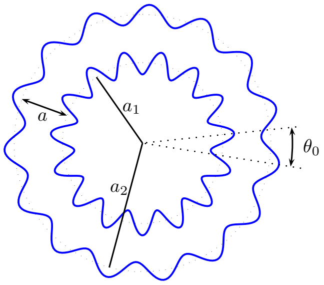

FIG. 1: Non-contact gears: Concentric corrugated cylinders with the same corrugation frequency, $\nu = 15$, on each cylinder. θ_0 is the angular shift between the gears.

Substituting the above expression into eq. (32), and taking the derivatives with respect to a_1 and a_2, we immediately perform the sum, leading to

$$L^{(2)W}_{mn} = \frac{\lambda_1\lambda_2}{8\pi}\frac{1}{a_2^2}\frac{\partial}{\partial\beta}\left[\frac{\beta^{m+n+1}}{1-\beta^2}\right] = -\frac{\lambda_1\lambda_2}{16\pi}\frac{1}{a^2}\,\alpha^2\frac{\partial}{\partial\alpha}\left[\frac{1}{\alpha}\left(\frac{1-\alpha}{1+\alpha}\right)^{m+n}(1-\alpha^2)\right], \qquad m\geq 0, n\geq 0, \tag{36}$$

where we have denoted $\beta = a_1/a_2$ for convenience. Interpreting $m/R \to k_1$ and $n/R \to k_2$, and taking the limit $m\to\infty$, $n\to\infty$, while keeping $k_{1,2}$ fixed, we obtain the expression for the L-kernel for corrugated plates in the weak limit [7].

IV. SINUSOIDAL CORRUGATIONS

For the particular case of sinusoidal corrugations, as described in figure 1, we will have

$$h_1(\theta) = h_1\sin[\nu(\theta+\theta_0)], \tag{37a}$$
$$h_2(\theta) = h_2\sin[\nu\theta], \tag{37b}$$

where $h_{1,2}$ are the corrugation amplitudes and ν is the frequency associated with the corrugations. Necessarily, ν must be a positive integer. The Fourier transforms, $(\tilde{h}_i)_m$, corresponding to the above corrugations are

$$(\tilde{h}_1)_m = h_1\frac{2\pi}{2i}\left[e^{i\nu\theta_0}\delta_{m,\nu} - e^{-i\nu\theta_0}\delta_{m,-\nu}\right]. \tag{38}$$

In general the corrugation frequencies of the two cylinders can be different. However, we note that, to the leading order, the interaction energy gets contributions only when both cylinders have the same frequency.

Using the above expression in eq. (18) and using the symmetry property of $I^{(2)}_{mn}$ in eq. (22), which further lets us deduce $L^{(2)}_{mn} = L^{(2)}_{nm}$, we can write

$$\frac{E^{(2)}_{12}}{L_z} = \cos(\nu\theta_0)\,\frac{h_1h_2}{2}\sum_{m=-\infty}^{\infty}L^{(2)}_{m,m+\nu} = -\cos(\nu\theta_0)\,\frac{h_1h_2}{8\pi}\sum_{m=-\infty}^{\infty}\int_0^\infty \kappa\, d\kappa\, I^{(2)}_{m,m+\nu}(a_1,a_2;\kappa) \tag{39}$$

where the kernel has been explicitly evaluated in eq. (23).

A. Dirichlet Limit

In the Dirichlet limit the interaction energy in eq. (39) can be expressed in the form

$$\frac{E^{(2)}_{12}}{2\pi R\, L_z} = \cos(\nu\theta_0)\,\frac{\pi^2}{240\,a^3}\,\frac{h_1}{a}\frac{h_2}{a}\,B^{(2)D}_\nu(\alpha) \tag{40}$$

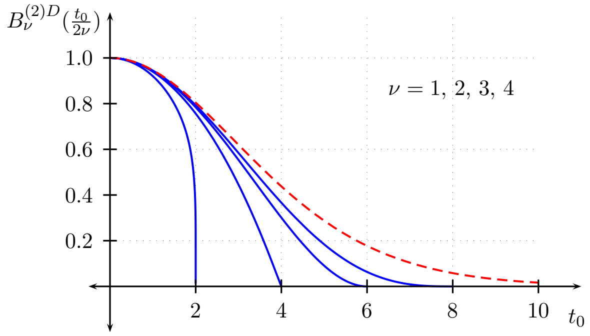

FIG. 2: Dirichlet limit: Plots of $B_\nu^{(2)D}(\frac{t_0}{2\nu})$ versus t_0, for $t_0 < 2\nu$ and fixed ν. The dashed curve is the corresponding plot for corrugated plates which is approached by the corrugated cylinders for larger values of ν.

where we have divided by a factor of $2\pi R$, which is the mean circumference in the direction of corrugations. We have also defined a suitable function $B_\nu^{(2)}(\alpha)$ to make it convenient to compare our results with those obtained in the PFA limit and with those for corrugated plates in the appropriate limits. We define

$$B_\nu^{(2)D}(\alpha) = \frac{15}{\pi^4} \sum_{m=-\infty}^{\infty} 8\alpha^3 \int_0^\infty x\,dx \frac{4\,\alpha^2}{(1-\alpha^2)} \frac{1}{D_m(\alpha;x)} \frac{1}{D_{m+\nu}(\alpha;x)}. \tag{41}$$

Using eq. (29) it is straightforward to verify the corrugated plate limit of the above expression. The function $B_\nu^{(2)D}(\alpha)$ has been plotted with respect to $t_0 = 2\alpha\nu$ in figure 2. The redefined parameter helps us compare our results with the corrugated plates. We note that for larger values of ν the plots approach the curve for the corrugated plates very quickly. We note that $B_\nu^{(2)D}(1) = 0$, because for $\alpha = 1$ the radius of the inner cylinder approaches zero. Thus, it is pointless to consider the regime $\alpha > 1$. We also note that $B_\nu^{(2)D}(0) = 1$, which then implies the PFA limit.

The Casimir torque per unit area, for the Dirichlet case, can thus be evaluated, using eq. (40) in eq. (4), to be

$$\frac{\mathcal{T}^{(2)D}}{2\pi R\, L_z} = \nu \sin(\nu\theta_0)\, \frac{\pi^2}{240\, a^3}\, \frac{h_1}{a} \frac{h_2}{a}\, B_\nu^{(2)D}(\alpha). \tag{42}$$

B. Weak coupling limit

The evaluation for the L-matrix in the weak limit in eq. (36) is valid for positive indices only. Therefore, we begin by rewriting the expression for the interaction energy in eq. (39) in the form

$$\frac{E_{12}^{(2)W}}{L_z} = \cos(\nu\theta_0)\, \frac{h_1 h_2}{2} \left[2 \sum_{m=0}^{\infty} L_{m,m+\nu}^{(2)W} + \sum_{m=1}^{\nu-1} L_{m,\nu-m}^{(2)W} \right], \tag{43}$$

where the finite sum is interpreted as zero when $\nu = 1$. We have used the symmetry property mentioned before eq. (39), and further used $L_{m,n}^{(2)W} = L_{-m,n}^{(2)W} = L_{m,-n}^{(2)W} = L_{-m,-n}^{(2)W}$, which can be deduced from eq (31) using the Bessel function property $I_{-m}(x) = I_m(x)$ and $K_{-m}(x) = K_m(x)$. After substituting the L-matrix, derived in eq. (36), into the above equation we can immediately perform the sums to yield

$$\frac{E_{12}^{(2)W}}{2\pi R\, L_z} = \cos(\nu\theta_0)\, \frac{\lambda_1\lambda_2}{32\pi^2\, a}\, \frac{h_1}{a} \frac{h_2}{a}\, B_\nu^{(2)W}(\alpha), \tag{44}$$

where we have defined the function

$$B_\nu^{(2)W}(\alpha) = -\frac{\alpha^3}{2} \frac{\partial}{\partial\alpha} \left[\frac{1}{\alpha^2} \left(\frac{1-\alpha}{1+\alpha} \right)^\nu (1-\alpha^2)(1+2\alpha\nu+\alpha^2) \right]. \tag{45}$$

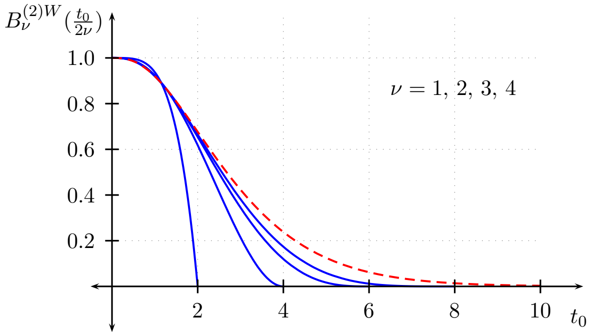

FIG. 3: Weak coupling limit: Plots of $B_\nu^{(2)W}(\frac{t_0}{2\nu})$ versus t_0, for $t_0 < 2\nu$ and fixed ν. The dashed curve is the corresponding plot for corrugated plates which is approached by the corrugated cylinders for larger values of ν.

The Casimir torque per unit area, for the weak coupling limit, can thus be evaluated, using eq. (44) in eq. (4), to be

$$\frac{\mathcal{T}^{(2)W}}{2\pi R\, L_z} = \nu \sin(\nu\theta_0)\, \frac{\lambda_1\lambda_2}{32\pi^2\, a}\, \frac{h_1}{a}\, \frac{h_2}{a}\, B_\nu^{(2)W}(\alpha). \tag{46}$$

We note that $B_\nu^{(2)W}(0) = 1$. This verifies that the above result satisfies the proximity force theorem. As in the Dirichlet case, we note that $B_\nu^{(2)W}(1) = 0$, because for $\alpha = 1$ the radius of the inner cylinder approaches zero. The above result should also yield the result for corrugated parallel plates in the limit $\nu \to \infty$, $a_{1,2} \to \infty$, $R \to \infty$, such that a and ν/R is finite. Also, in this limit $\alpha \to 0$. Recalling the corrugated plates parameter [7], $k_0 a \to \nu a/R = 2\nu\alpha \equiv t_0$, we note that the limit to corrugated plates is achieved by taking the limit $\nu \to \infty$ with t_0 kept fixed. To this end we rewrite eq. (45) in terms of t_0 as

$$B_\nu^{(2)W}\left(\frac{t_0}{2\nu}\right) = -\frac{t_0^3}{2}\frac{\partial}{\partial t_0}\left[\frac{1}{t_0^2}\left(1-\frac{t_0}{2\nu}\right)^\nu \left(1+\frac{t_0}{2\nu}\right)^{-\nu}\left(1-\frac{t_0^2}{4\nu^2}\right)\left(1+t_0+\frac{t_0^2}{4\nu^2}\right)\right] \tag{47}$$

in which the $\nu \to \infty$ limit can be immediately taken to yield

$$\lim_{\nu\to\infty} B_\nu^{(2)W}\left(\frac{t_0}{2\nu}\right) = -\frac{t_0^3}{2}\frac{\partial}{\partial t_0}\left[\frac{1}{t_0^2}(1+t_0)\, e^{-t_0}\right] = \frac{t_0^3}{2}\frac{\partial^2}{\partial t_0^2}\left[\frac{1}{t_0}\, e^{-t_0}\right], \tag{48}$$

which matches the result for the corrugated plates exactly. The function $B_\nu^{(2)W}(\alpha)$ has been plotted with respect to t_0 in figure 3. As in the case of Dirichlet case, we note that for larger values of ν the plots approach the plot for corrugated plates very quickly.

V. CONCLUSION AND FUTURE DIRECTIONS

We have evaluated the Casimir torque between two concentric corrugated cylinders perturbatively in the corrugation amplitude for the scalar case. We have derived explicit expressions for the case when the cylinders have sinusoidal corrugations. Nonzero contributions in the leading order requires the corrugation frequencies on the two cylinders to be identical. Our results for the Casimir torque reproduce the results for the lateral force on corrugated parallel plates in the limit of large radii and small corrugation wavelengths.

Extension of the calculation to the next-to-leading order in the spirit of [7] is in progress. We recall that it was possible to evaluate the lateral force between corrugated parallel plates, in the weak limit, exactly in terms of a single integral [7]. The corresponding exact result for the Casimir torque between corrugated cylinders, in the weak limit, is being sought. Generalization to the electromagnetic case is most important and we intend to attempt it next. Generalization of the calculation to the case of a rack and pinion arrangement is another possible extension. We hope that these calculations will have application in the design of practical nanomechanical devices.

Acknowledgments

We thank Jef Wagner for extensive collaborative assistance throughout this project. We thank the US National Science Foundation (Grant No. PHY-0554926) and the US Department of Energy (Grant No. DE-FG02-04ER41305) for partially funding this research. ICP would like to thank the French National Research Agency (ANR) for support through Carnot funding.

[1] H. B. G. Casimir, Kon. Ned. Akad. Wetensch. Proc. **51** (1948) 793.
[2] Yu. S. Barash, Izv. Vuzov. Ser. Radiofiz. **16**, 1086 (1973) [Sov. Radiophys. **16**, 945 (1973)].
[3] S. J. van Enk, Phys. Rev. A **52**, 2569 (1995).
[4] T. Emig, A. Hanke, R. Golestanian and M. Kardar, Phys. Rev. Lett. **87**, 260402 (2001) [arXiv:cond-mat/0106028].
[5] A. Ashourvan, M. Miri, and R. Golestanian, Phys. Rev. Lett. **98**, 140801 (2007).
[6] F. C. Lombardo, F. D. Mazzitelli and P. I. Villar, J. Phys. A **41**, 164009 (2008) [arXiv.org:0801.4551 [quant-ph]].
[7] I. Cavero-Pelaez, K. A. Milton, P. Parashar and K. V. Shajesh, arXiv:0805.2776 [hep-th].
[8] T. Emig, N. Graham, R. L. Jaffe and M. Kardar, Phys. Rev. D **77**, 025005 (2008) [arXiv:0710.3084 [cond-mat.stat-mech]].
[9] K. A. Milton and J. Wagner, J. Phys. A **41**, 155402 (2008) [arXiv:0712.3811 [hep-th]].
[10] M. Abramowitz and I. A. Stegun, Editors, *Handbook of Mathematical Functions with Formulas, Graphs, and Mathematical Tables* (Dover, New York, 1964, ninth Dover printing, tenth GPO printing), Secs. 9.7.7, 9.7.8.